

Probing the Merger in ACT-CL J0256.5+0006: Understanding Low-Power Radio Halos

Author: Colin Sullivan

Instructor: Craig Sarazin

5/10/2019

The University of Virginia's Department of Astronomy

This thesis is submitted in partial completion of the requirements of the BS Astronomy-Physics Major.

Probing the Merger in ACT-CL J0256.5+0006: Understanding Low-Power Radio Halos

ABSTRACT

ACT-CL J0256.5+0006 (J0256) is a moderate redshift ($z=0.363$) merging cluster. Around it, one of the weakest known cluster giant radio halos has been observed. Based on our ACT SZ detection and a very short XMM observation, J0256 has the weakest SZ and possibly the lowest mass ever observed for a radio halo as well. Our Chandra observation gives J0256’s dynamical merger state: it is an early-stage merger, which challenges the theory that radio halos are produced by turbulent re-acceleration after the passage of merger shocks. It is also possible that this merger is a late-stage merger, and the observed structures are simply due to projection effects caused by the merger’s orientation with respect to our line of sight. This possibility will also be investigated.

1. INTRODUCTION

The cluster merger J0256 is interesting because previous observations such as those from [Majerowicz et al. \(2004\)](#) have shown it to be an unusually low-mass merger, but more importantly they have detected an extremely weak cluster giant radio halo around it. Radio halos are roughly symmetric sources with steep radio spectra, a projection onto a cluster’s center ([Deiss 1997](#)), and no clear optical counterpart ([Willson 1970](#); [Feretti et al. 2012](#)). They are most commonly found in merging clusters and it is thus believed that the radio-emitting electrons are being accelerated by merger-driven processes, such as shock waves (e.g., [Feretti et al. 2012](#)).

This paper investigates the reason that J0256’s radio halo is especially weak, and attempts to discover whether it is simply a product of the merger’s low mass ([Russell et al. 2011](#)), a result of the merger still being in its early stages ([Cassano 2010](#)), or a consequence of some other, unforeseen factor. This is done by evaluating the large gas structures observed within the clusters as well as their temperature gradients, which are determined based on the concentration of hard, medium, and soft X-rays throughout the cluster. By observing the structures present within the merger, it is possible to determine if the two clusters have already passed each other, which would mean that it is no longer in its early stage. The temperature gradient can show any cold fronts or particularly energetic regions, which are also indicators of merger stages. Later-stage mergers will have already disrupted the cool cluster cores, whereas early stage mergers will likely still have their cores intact.

2. OBSERVATIONS AND DATA REDUCTION

J0256 was observed with the Chandra X-ray Observatory in two closely-spaced periods using the ACIS-S detectors. The properties of the two observations are given in Table 1.

The data were analyzed using the the *Chandra Interactive Analysis of Observations* (CIAO) software system (version 4.11) with CALDB version 4.8.2¹, as well as HEASoft version 6.24².

We reprocessed the level-1 events files using the CIAO CHANDRA_REPRO command to ensure that up-to-date and consistent calibrations were applied. The data were corrected for afterglows, bad pixels, charge transfer inefficiency, and the time-dependent gain.

The cluster is mainly located on the S3 (chip 7) CCD, which is back-side illuminated. The light-curve (energy band 0.5–7 keV) from the source-free region of the S1 (chip 5) detector was used to filter out times of increased background (“background flares”). The background light-curves for chips 6 and 7 are shown in Figure 1. S1 is also a back-side illuminated CCD, and gave slightly better statistics since the cluster region did not need to be excluded on it. The background flares were removed with the CIAO DEFLARE command using the “clean” method. Both the raw and the resulting cleaned exposure times for the S3 chip are given in Table 1.

Blank-sky background events files were created using CIAO’s BLANKSKY tool, which tailors the background file to the aspect history of the observation. The blank-sky background were scaled by the number of events in

¹ <http://cxc.harvard.edu/ciao/>

² <https://heasarc.gsfc.nasa.gov/docs/software/heasoft/>

OBSID	Date	RA	Dec	Roll Angle ($^{\circ}$)	Exposure:	
					Raw (ks)	Clean (ks)
20531	2017-11-30	2h 56m 34.7s	0 $^{\circ}$ 6' 27.87"	320	42.55	39.92
20868	2017-12-01	2h 56m 34.8s	0 $^{\circ}$ 6' 27.51"	320	25.77	23.98

Table 1. Observation Data

the 9.0-12.0 keV band, which is dominated by particle background.

For the purposes of imaging, the cleaned events files from the two observations were merged using the CIAO tool `MERGE_OBS`. We adopted the coordinates of the longer OBSID 20531, and shifted the shorter OBSID 20868 to match this. Note that the two observations have the same roll angle, but that the pointing locations were displaced by about 4 pixels along the axis of the ACIS-S detector. This shift acts to further wash out exposure variations, along with the normal nodding motion of *Chandra*. Point sources in the merged images were checked to ensure the two observations were aligned correctly.

The cluster is entirely contained on the S2 and S3 CCDs (chips 6 and 7). Thus, we will restrict the remaining analysis to these two detectors. Figure 2 shows a raw image (uncorrected for background or exposure) of the S2 and S3 chips to show the geometry of the data. The J0256 cluster is near the lower left edge of the upper S3 chip, and is double with strong concentrations at the centers of the two subclusters.

The point sources in the merged 0.5–7.0 keV image were detected using the CIAO command `WAVDETECT`. The variation in the ACIS point-spread-function (PSF) across the field was included. The PSFs from the two observations were determined, and were merged, weighting by the exposure map for each observation. We adopted

a source threshold of 10^{-6} , and used wavelet sizes of 1, 2, 4, 8, 16, and 32 pixels. The resulting source list was inspected for false, missing, and extended sources. The remaining sources were then removed from the list, and therefore excluded from most images. Extended sources that appeared to be part of the cluster were not excluded.

With the point sources removed, the resulting images were adaptively smoothed using the CIAO `CSMOOTH` command. This smoothing process involved correcting the images for both background and exposure. The smoothed image allowed us to determine features of the merger that were previously unseen, and this image is displayed in Figure 3. This source-removal and smoothing process was initially conducted on the broad band observation files, and then repeated for the hard, medium, and soft band files individually. The bands corresponded to energy ranges of 2-7keV, 1.2-2keV, and 0.5-1.2keV respectively. One key difference between the way the broad and individual band images were processed is that each of the individual band images was smoothed according to the broad image’s specific smoothing scale. This was to ensure a uniform smoothing across the three images and therefore general consistency throughout the data, with the broad image’s smoothing scale being chosen because it was a combination of all three individual bands. Once these three bands were processed individually, they were combined to form an RGB image in the image-processing software, DS9. Soft X-rays were loaded in as red, medium as green, and hard as blue.

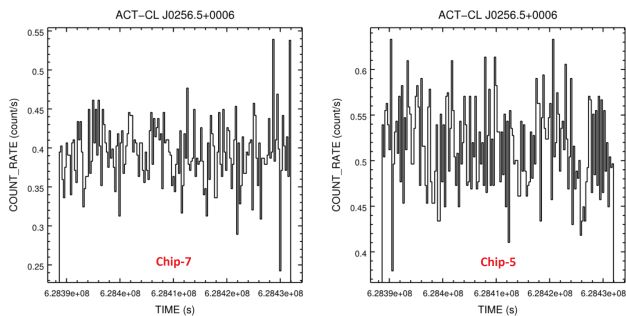


Figure 1. Background light-curves from OBSID 20531 for the two back-side-illuminated CCDs in the 0.5-7 keV band. The two curves have different Count Rate scales, with Chip-5’s values ranging from 0.38-0.62, and Chip-7’s values only ranging from 0.23-0.54. *Left:* S3 or Chip-7, which contains the center of the cluster. *Right:* S1 or Chip-5, which was used to remove flares.

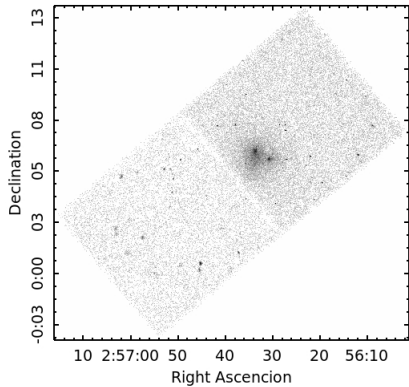


Figure 2. Raw image (not corrected for background or exposure) from the merged data for the S3 (Chip-7, upper right) and S2 (Chip-6, lower left) CCDs. The image was smoothed with a gaussian kernel with a width of $\sigma = 3$ pixels ($1''.49$) to make it easier to see the point sources.

3. DISCUSSION

One of the goals of this observation was to discover the temperature structure of the clusters. This was done with the RGB image created by combining the three different X-ray band observations. See Figure 4. These different energy bands were used to map temperature because as the temperature of gas increases, the X-rays that the gas emits increase from the soft band to the hard band. This means that in our image, the more red an area is, the cooler the gas, and the more blue, the hotter the gas. It is clear that large amounts of radiation in all three bands are being emitted in the center of each cluster, as the image is saturated. Immediately outside the center the gas is noticeably cool, however, and from that point out the gas becomes hotter and less dense the further it is away from the center. Around the edges there is a region composed entirely of hot, diffuse gas.

The most prominent features of the merger are a possible shock or cold front between the two clusters, and a tail of gas behind each cluster. The eastern cluster's tail is trailing from north to south, and the western cluster's tail is trailing from east to west. This orientation tells us that the merger is not happening strictly in plane-of-sky directions, because if the western cluster were moving directly east then the eastern cluster would not yet have formed a tail. This conclusion is in turn drawn from the fact that information in gas cloud turbulence cannot travel faster than the speed of a shock wave, and therefore the tail of the eastern cluster could not have been shaped by anything in front of the shock wave. With these facts established, the question of why the eastern cluster has a tail at all is raised. The only

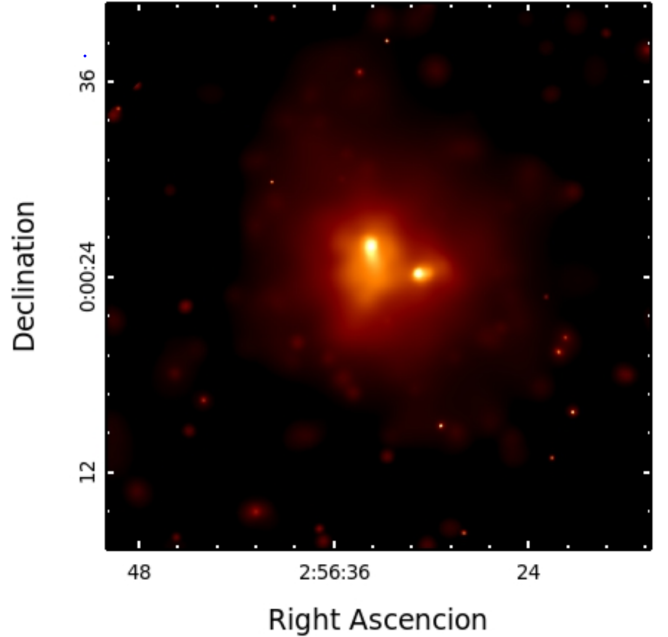


Figure 3. An adaptively smoothed image of the combined broad spectrum data. It is particularly useful for visualizing the general gas structures in the merger, including tails and the front at which the two clusters are meeting.

explanation is that there are movements occurring in directions outside the plane of the sky.

Previous observations of redshift in this merger have discovered a clear distinction between the two clusters: while the galaxies in the eastern cluster has an average redshift of approximately 0.361, the galaxies in the western cluster has an average redshift of approximately 0.368. This difference in redshift correlates to a difference in line-of-sight velocity of roughly 1500km/s, which is substantial (Sifn et al. 2016). There are two primary explanations of this difference: either the western cluster is closer to us and accelerating away towards the eastern cluster, or the western cluster is not actually merging with the eastern cluster at all but rather is simply a separate object that is significantly further away from us and thus has a higher Hubble redshift.

While the idea that the western cluster is a completely separate object with a higher Hubble redshift easily explains the difference in relative velocities, it does nothing to explain the features that are observed in our images. If these two clusters are not merging, then there is nothing to explain why either one of them has a tail, let alone why they both have tails that appear on a similar size scale. For the western cluster to be significantly further away, while having the angular width that we observe, it would have to be much, much larger than the eastern cluster. This theory also has no way of explaining the observed shock/cold front that is observed between

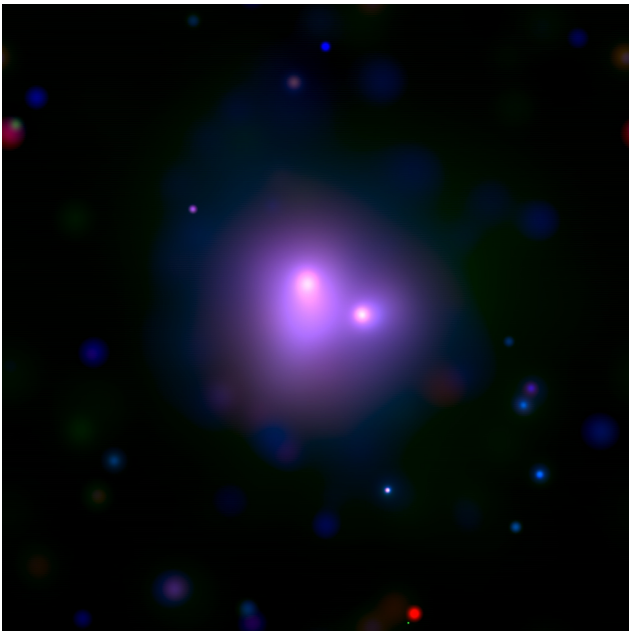


Figure 4. RGB image of the merger, with red representing smooth X-rays, green representing medium X-rays, and blue representing hard X-rays.

the two clusters, and thus is not worth considering. It is much more likely that the western cluster is accelerating away from us towards the eastern cluster, as this suggests that the merger is happening mostly in the line of sight. This in turn supports the previous assertion that the observed cluster structures are being caused by interactions that are taking place outside of the plane of the sky.

Further evidence that this merger is still in its early stages can be found in the lower-temperature cluster cores. A common characteristic of later-stage mergers is that the merging clusters' initially cool cores will have become less defined and induced cold fronts that propagate through the merger. The lack of a noticeable cold front, combined with the undisturbed cold cores in the center of each cluster, suggest that this merger is still in its early stages.

The only evidence supporting the idea that this merger is in its later stages is the tail of the eastern cluster. Assuming that this merger is in its early stages, it is hard to explain why the eastern cluster has such a pronounced North to South tail. This is no harder to explain than why both cores would still be perfectly intact during the later stages of a merger, however.

4. CONCLUSION

Throughout this investigation, efforts were made to determine the cause of the merger ACT-CL J0256.5+0006's exceptionally weak radio halo. We were unable to quan-

tify the effect that the clusters' low masses may have on the radio halo, but we have presented substantial evidence for the claim that J0256 is an early-stage merger. This evidence is broken up into two main points: the clusters' cool cores are intact, and the clusters' tails indicate that a first pass has not yet occurred.

After the first pass in a merger, the cool cores that are common in clusters often get disturbed and lose their distinct, circular shapes. When this disturbance occurs, the cool gas in the cores is often projected out to form a cold front that travels through the cloud. There is only one structure in our image that can be interpreted as a cold front, and it is much more likely to be a shock front or some such structure which appears as it does because of the merger's orientation with respect to the plane of the sky. This is the case because in the temperature structure that we deduced, the only sharp gradients present are those just outside of each cluster's circular core. In these new smoothed images, it is obvious that the eastern cluster has a tail that flows from North to South and the western cluster has a tail that flows East to West. If the merger were taking place in the plane of the sky, which is the intuitive conclusion from first glance, then these tails would be inexplicable. Instead, based on the relative velocities that were described in (Sifón and et al. 2017), it is clear that the western cluster is traveling away from Earth and towards the eastern cluster in a trajectory that falls primarily within our line of sight. Thus the merger is not happening primarily in the plane of the sky due to multiple factors, including the roughly 1500 km/s difference in line-of-sight velocities and the direction of the clusters' tails.

The presence and orientation of these tails also serve as evidence that the merger is still in its early stages. The fact that each cluster's tail is pointing away from the other cluster means that they are still heading towards their first pass. After the first pass, the clusters and their tails will begin to curve back towards each other for a second pass; at that point, both tails will be curved and pointing towards the other cluster. This is clearly not yet the case.

Based on the evidence presented, it seems conclusive that the merger ACT-CL J0256.5+0006 is an early-stage merger. This fact challenges the idea that radio halos are solely produced by re-acceleration of electrons after the initial passage of merger shocks, and reinforces the possibility that they are produced by some other merger-driven process instead. Further investigation into the clusters' masses and spectra should still be conducted in order to more completely understand the causes behind the presence and strength of radio halos.

REFERENCES

- R. Cassano. The radio-X-ray luminosity correlation of radio halos at low radio frequency. Application of the turbulent re-acceleration model. *A&A*, 517:A10, July 2010. <https://doi.org/10.1051/0004-6361/200913622>.
- B. M. Deiss. A deprojection method to obtain the spectral index distribution in diffuse radio halos of clusters of galaxies. *A&A*, 325:74–80, September 1997.
- L. Feretti, G. Giovannini, F. Govoni, and M. Murgia. Clusters of galaxies: observational properties of the diffuse radio emission. *A&A Rev*, 20:54, May 2012. <https://doi.org/10.1007/s00159-012-0054-z>.
- S. Majerowicz, D. M. Neumann, A. K. Romer, R. C. Nichol, D. J. Burke, and C. A. Collins. jASTROBJ_iRX J0256.5+0006_i/ASTROBJ_i: A merging cluster of galaxies at $z = 0.36$ observed with XMM-NEWTON. *A&A*, 425:15–32, October 2004. <https://doi.org/10.1051/0004-6361:20048005>.
- H. R. Russell, R. J. van Weeren, A. C. Edge, B. R. McNamara, J. S. Sanders, A. C. Fabian, S. A. Baum, R. E. A. Canning, M. Donahue, and C. P. O’Dea. A merger mystery: no extended radio emission in the merging cluster Abell 2146. *MNRAS*, 417:L1–L5, October 2011. <https://doi.org/10.1111/j.1745-3933.2011.01098.x>.
- C. Sifón and et al. VizieR Online Data Catalog: 44 SZ-selected galaxy clusters ACT observations (Sifon+, 2016). *VizieR Online Data Catalog*, 746, November 2017.
- M. A. G. Willson. Radio observations of the cluster of galaxies in Coma Berenices - the 5C4 survey. *MNRAS*, 151:1–44, 1970. <https://doi.org/10.1093/mnras/151.1.1>.